

# *Modeling the effect of EGR on combustion and pollution of dual fuel engines with flow field model*

\*Samad Jafarmadar<sup>1</sup>, Alborz Zehni<sup>2</sup>

<sup>1</sup>University of Urumia, Iran

<sup>2</sup>University of Tabriz, Iran

Received Date:30Aug; 2010

Accepted:31Oct; 2010

## **ABSTRACT**

At the present work, the effect of cold exhaust gas recirculation (EGR) on combustion and pollution of a dual fuel engine has been investigated by CFD code FIRE. The turbulent flow within the combustion chamber is simulated using the k- $\epsilon$  turbulence model, which is modified for engine flows. "Wave" and "Eddy break up" models are employed to predict combustion and spray process. The calculations carried out at the engine speed of 1400rpm and full load mode. The EGR percentage is from zero to 15. The results show that 10% EGR can reduce emissions significantly in comparison with the other cases. The predicted values of cylinder pressure and NOx emission of diesel and dual mode in the baseline state (without EGR) show a good agreement with the experimental data.

## **KEYWORDS**

EGR, dual fuel engine, combustion, NOx.

## **1. INTRODUCTION**

In dual fuel CI engines operating with natural gas as primary fuel and a "pilot" amount of liquid Diesel fuel as an ignition source, the gaseous fuel is inducted along with the intake air and is compressed like in a conventional Diesel engine. The mixture of air and gaseous fuel does not auto ignite due to its high auto ignition temperature. A small amount of liquid Diesel fuel is injected near the end of the compression stroke to ignite the gaseous mixture. Diesel fuel auto ignites and creates ignition sources for the surrounding air-gaseous fuel mixture. The pilot liquid fuel, which is injected by the conventional Diesel injection equipment, normally contributes only a small fraction of the engine power output [1].

The compression ignition engine of the dual fuel type has been employed in a wide range of applications to utilize various gaseous fuel resources and minimize exhaust gas emissions

without excessive increase in cost from that of conventional Diesel engines [2].

Although due to the existence of natural gas, dual fuel engines have the lowest Soot emissions, the NOx emission can be as high as diesel engines.

EGR is one of the most effective methods of controlling NOx emissions in dual fuel engines [3, 4, 5, and 6]. It involves the diversion of some of the exhaust gases back to the engine inlet system. In effect, the replacement of a small quantity of oxygen and nitrogen in the inlet air to the engine with carbon dioxide, vapor, burned and unburned hydrocarbons from the exhaust occurs. Since the specific heat capacity of carbon dioxide, water vapor and hydrocarbons is greater than that for oxygen, the gas temperature within the engine cylinder during combustion is reduced. In addition a reduction in the oxygen concentration at the flame region reduces the flame temperature. Considering that, thermal NOx concentration strongly depends on the

---

\* Corresponding author: S.Jafarmadar(e-mail:s.jafarmadar@Urmia.ac.ir)

oxygen and temperature, these reductions in oxygen concentration and flame temperature lead to a reduction in the NO<sub>x</sub> formation rate and NO<sub>x</sub> level in the exhaust.

Nowadays, the progressively more and tighter pollutant emissions regulations and fuel economy standards deeply affect internal combustion engine design and production process. In this field, computational tools like CFD play a fundamental role [7]. However in the case of the effects of EGR, regardless of the thermodynamic models and experimental works, the majority of the CFD researches has been confined to diesel engines [7, 8, 9]. Hence, at the present work, the effect of cold exhaust gas recirculation (EGR) on combustion and pollution of a dual fuel engine has been investigated by CFD code. The calculations are at the engine speed of 1400rpm and full load mode. The different EGR cases are from zero to 15%.

## 2. MODEL FORMULATION

### 2.1. FLOW FIELD MODEL

Based on the RANS equations and SIMPLE algorithm, the standard k-ε model has been used to simulate the flow field model [10].

### 2.2. IGNITION AND COMBUSTION MODELS

The “Shell” model [11] was used for ignition kinetics modeling. The model uses a reduced kinetic mechanism which contains five generic species and eight generic reactions to simulate the auto ignition phenomena of hydrocarbon fuels. “Eddy break up” model has been used for combustion modeling. This model assumes that in premixed turbulent flames, the reactants (fuel and oxygen) are contained in the same eddies and are separated from eddies containing hot combustion products. The rate of dissipation of these eddies determines the rate of combustion.

$$\overline{\rho r_{fu}} = \frac{C_{fu}}{\tau_R} \overline{\rho} \min \left( \overline{y_{fu}}, \frac{\overline{y_{ox}}}{S}, \frac{C_{pr} \overline{y_{pr}}}{1+S} \right) \quad (1)$$

$C_{fu}$  and  $C_{pr}$  are empirical coefficients and  $\overline{y_{pr}}$  is the turbulent mixing time scale for reaction. The value of the empirical coefficient  $C_{fu}$  has been shown to depend on turbulence and fuel parameters. Hence,  $C_{fu}$  requires adjustment with respect to the experimental combustion data for

the case under investigation.  $\overline{y_{pr}}$  is product mass fraction that which includes intermediate species, CO<sub>2</sub> and H<sub>2</sub>O.

The first two terms of the “minimum value of” operator determine whether fuel or oxygen is present in limiting quantity, and the third term is a reaction probability, which ensures that the flame is not spread in the absence of hot products.

### 2.3. SPRAY MODEL

The “Wave” standard model [12] is used for droplet break up modeling. In this model the growth of an initial perturbation on a liquid surface is linked to its wave length and to other physical and dynamic parameters of the injected fuel and the domain fluid. Drop parcels are injected with characteristic size equal to the nozzle exit diameter. The differential equation of the reduction of the initial droplet diameter can be written as:

$$\frac{dr}{dt} = \frac{-(r - r_{stable})}{t} \quad (2)$$

$$r_{stable} = c_1 \Lambda \quad (3)$$

Which

$$t = c_2 \cdot \frac{r}{w} \left( \frac{\rho_l}{\rho_g} \right)^{\frac{1}{2}} \quad (4)$$

$c_1$  and  $c_2$  are constants which are equal to 0.61 and 12. The heat and mass transfer process are described by a model which is derived by “Dokowicz” [13]; with the assumption of uniform droplet temperature, the rate of droplet temperature change is determined by the energy balance equation, which states that the energy conducted to the droplet either heats up the droplet or supplies heat for vaporization.

$$m_d c_{pd} \frac{dT_d}{dt} = L \frac{dm_d}{dt} + \dot{Q} \quad (5)$$

The convective heat flux supplied from the gas to the droplet surface is:

$$\dot{Q} = \alpha A_s (T_\infty - T_s) \quad (6)$$

Spray wall interaction model is “Walljet1” [14] which assumes that under engine conditions, a vapour cushion is formed under the droplets and that they rebound or slide along the walls, depending on the Weber number. The transition criterion between these

two regimes is described by a critical Weber number which is taken to be  $We_c=80$ .

## 2.4. EMISSION MODELS

The thermal NO formation mechanism is expressed in terms of the extended zeldovich mechanism.

The conservation equation for NO is expressed as:

$$\frac{d[NO]}{dt} = 2k_f[N_2][O_2] \quad (7)$$

Which

$$k_f = \frac{A}{\sqrt{T}} \exp\left(\frac{-E_a}{RT}\right) \quad (8)$$

The soot formation rate is modeled as the difference between soot formation [15] and soot oxidation [16]:

$$\frac{dm_{soot}}{dt} = \frac{dm_{form}}{dt} - \frac{dm_{oxid}}{dt} \quad (9)$$

Where soot formation rate is:

$$\frac{dm_{form}}{dt} = A_f m_{fv} P^{0.5} \exp\left(-\frac{E_a}{RT}\right) \quad (10)$$

with  $A_f$  as the pre exponential factor,  $m_{fv}$  is the fuel vapor mass,  $P$  is the pressure and  $E_f$  is the activation energy.

Soot oxidation rate is:

$$\frac{dm_{oxid}}{dt} = \frac{6M_c}{\rho_s d_s} m_s R_{tot} \quad (11)$$

where  $M_c$  is the carbon molecular weight,  $\rho_s$  is the soot density,  $d_s$  is the average soot diameter,  $m_s$  is the soot mass and  $R_{tot}$  is the net reaction rate.

## 3. THREE DIMENSIONAL MODELING OF OM-355 DIESEL ENGINE

The characteristics of OM-355diesel engine is shown in table 1. In dual fuel mode, 90% of the diesel fuel is replaced by the natural gas (methane) and air mixture in the compression stroke. 10% of the pilot fuel (diesel) is used for the ignition source of the charge. To quantify the amount of EGR, the EGR percentage is defined by:

$$EGR(\%) = \left( \frac{\dot{m}_{EGR}}{\dot{m}_{EGR} + \dot{m}_{NG} + \dot{m}_{air}} \right) \quad (12)$$

Table 1  
The Characteristics Of Om-355 Mercedes-Benz Diesel Engine

Engine type	Heavy duty D.I. diesel engine
The number of injector holes	4
Engine speed at max torque	1400 rpm
Engine speed at max power	2200 rpm
Piston diameter*stroke	150*128mm
Cylinder volume	11.58L/6
Injection pressure	195 bar
Max out put power	240 hp
Max outlet torque	824 N.m
The number of cylinders	6,vertical type

The piston geometry and computational moving mesh can be observed in figure 1. A 90 degree sector mesh is used in this study considering that the diesel injector has four nozzle holes. The numerical calculations are from inlet valve closing until exhaust valve opening.

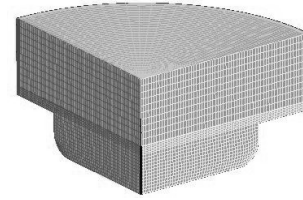


Fig.1: The 3D mesh of OM-355 diesel engine

## 3. RESULTS AND DISCUSSIONS

Figure 2 shows the heat release rate of dual fuel engine for different EGR cases. Two peaks can be seen from the diagram. The first peak is due to the ignition of the diesel fuel and the second peak is related to the premixed combustion of the natural gas and air mixture. As can be seen, EGR has little effect on ignition delay but causes premix combustion peaks to shrink in height with delayed timing. The reason is that the temperatures in cylinder are similar for all cases at before combustion. the lower oxygen mass fraction in intake gases due to EGR inevitably reduces the chance of the fuel mixing with oxygen, which in turn decreases the ratio of burning fuel to entire fuel, thus causing the burning ratio at certain time and at certain locations in the combustion chamber to decrease,

lowering the heat generation at that time, and retarding the rise in the combustion temperature. The elongation of diffusion combustion is also caused by the decrease in burning ratio, which in turn results from lower oxygen concentration. Since the combustion progresses more slowly, the diffusion combustion tends to propagate over a wide zone.

In the case of 15% cold EGR, the heat release rate becomes higher at the premixed combustion. The reason is probably due to the activation of the free radicals in the component of EGR gases as shown in equation (1) with  $\bar{y}_{pr}$  parameter.

Also this is probably because the increasing intermediate species became more significant than the dilution effect.

As can be seen in the figure 3, the delay of ignition in the case of 15% EGR is shorter and methane is consumed faster in comparison with the other cases.

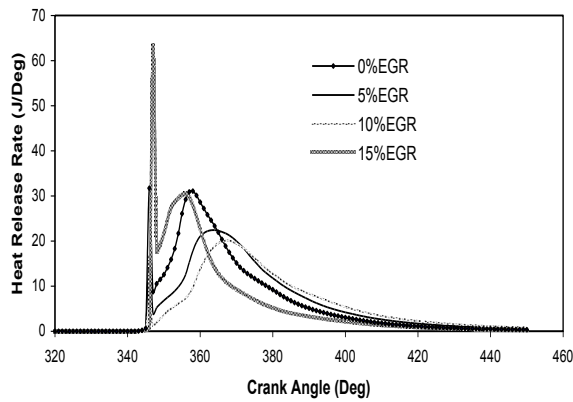


Fig.2: Variations of heat release rate with crank position for different EGR cases.

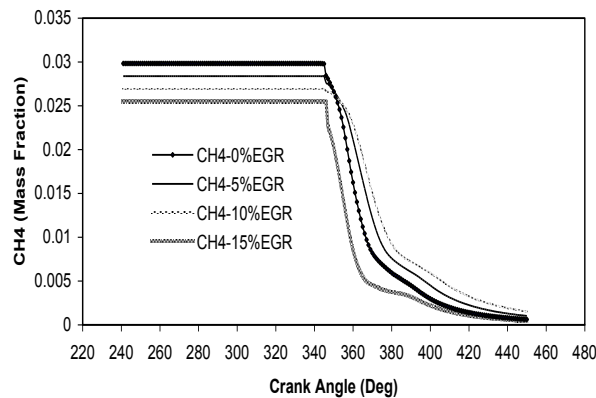


Fig.3: Variations of methane (natural gas) consumption with crank position for different EGR cases

Figure 4 and figure 5 show the in cylinder pressure and temperature of the dual fuel engine for different EGR cases. As can be seen, with increasing EGR, the cylinder pressure and temperature decreases. The difference between the values of pressure and the temperature In the case of 0% EGR (normal state) and 10% EGR are 2.22 Mpa and 340K, i.e. EGR can favorably control the rate of pressure and temperature rise. The unexpected behavior of the 15% EGR case can be expounded according to the above explanation for figure 2.

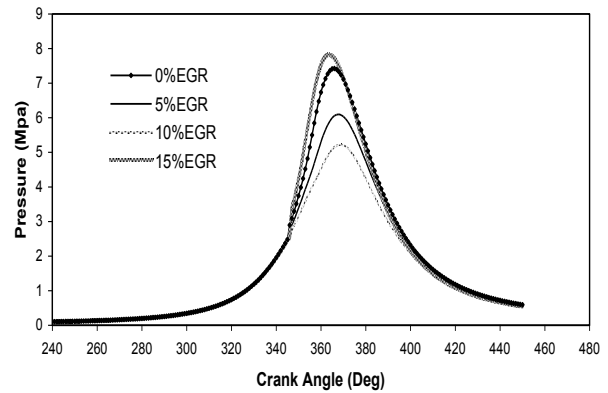


Fig. 4: Variations of the cylinder pressure with crank position for different EGR cases.

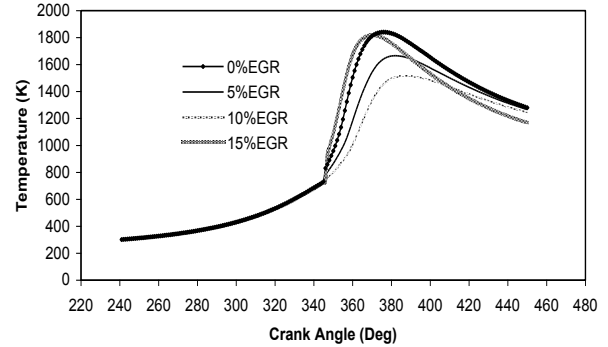


Fig.5: Variations of the cylinder temperature with crank position for different EGR cases.

Figure 6 shows the NOx emission for different EGR cases. It can be seen that with increasing EGR, NOx is reduced. The main result is related to the lower oxygen and temperature in the cylinder. In the case of the 15% EGR, the high temperature is the main reason for high NOx concentration.

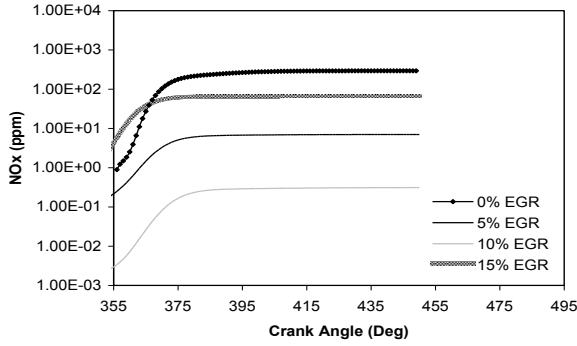


Fig.6: Variations of the NOx concentration with crank position for different EGR cases.

Figure 7 presents the Variations of the Soot concentration with crank position for different EGR cases. As can be seen, with increasing EGR, Soot emission decreases. The main reason can be due to the thermal and radical effects of EGR as shown which accelerates the oxidation of Soot. In the case of the 15% EGR, as can be seen from the figure 5, since after the peak of cylinder temperature, the decrease of temperature is faster in comparison with the other cases, the rate of oxidation is lower. Thermal effect, influences soot formation and oxidation directly as shown  $T$  in equation (15) and  $R_{tot}$  (net reaction rate) in equation (16)}. However, Radical effect influences soot formation indirectly and soot oxidation directly as shown  $R_{tot}$  in equation (16). I.e. it affects the thermal effect which leads to the soot variation.

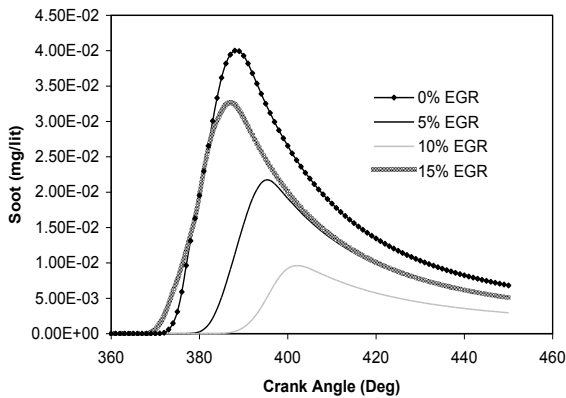


Fig.7: Variations of the Soot concentration with crank position for different EGR cases.

Figure 8 shows the contour plots of reaction progress variable for different EGR cases at different crank angle degrees. It can be observed that the more the higher EGR, the less the intense combustion. With the exception of 15% EGR

which as mentioned, the radical and thermal effects can be the main reasons for the more intense combustion.

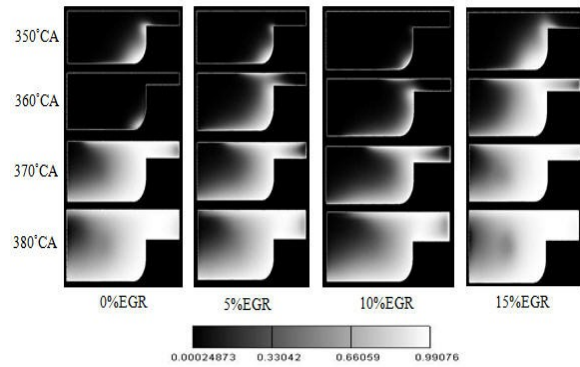


Fig.8: contours of reaction progress variable for EGR cases at different crank angle degrees.

Figure 9 presents the contour plots of NOx mass fraction for different EGR cases at exhaust valve opening position. It can be seen that for all the cases, NOx is concentrated into the bowl of the piston. The lower NOx concentration of the 10% EGR case, in comparison with the other EGR cases is evident.

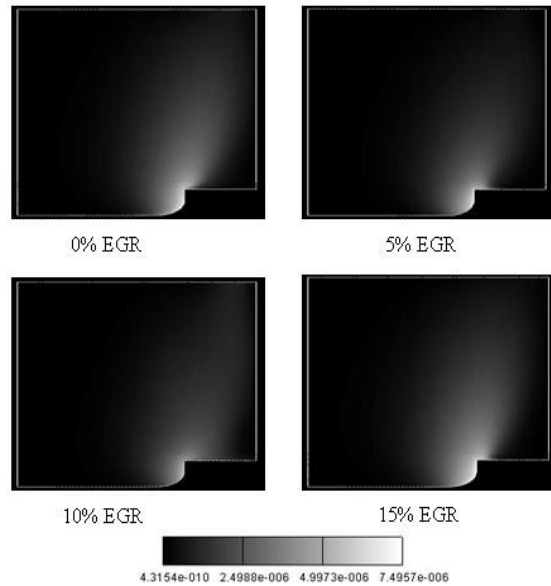


Fig.9: contour plots of NOx mass fraction for different EGR cases at Exhaust valve opening

Figure 10 reveals the contour plots of Soot mass fraction for different EGR cases at exhaust valve opening position. As can be seen, for all the cases, Soot is centralized to the top of the piston bowl space. The lower Soot concentration of the 10% EGR case, in comparison with the other EGR cases is evident in this figure too.

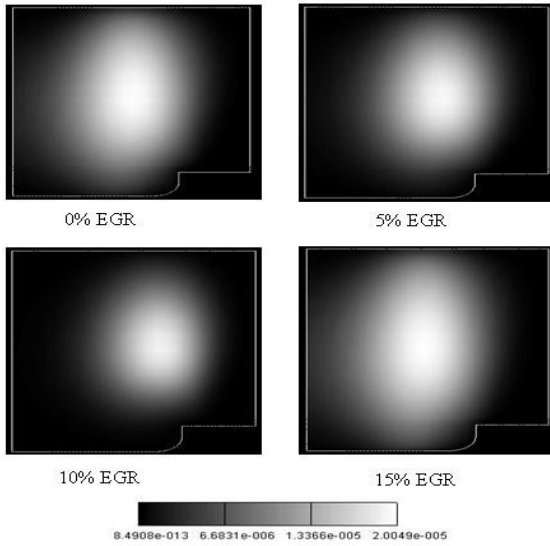


Fig.10: contour plots of Soot mass fraction for different EGR cases at Exhaust valve opening. According to the above observations and explanations, the best case of EGR in which the performance remains at a good level and pollution decreases significantly is 10%.

In order to validate the simulated model, figure 11 and figure 12 show the comparison of the in cylinder pressure and NOx level in both diesel and dual fuel modes with the experimental data [17]. The results are at normal mode of the engines i.e. without EGR and a good agreement can be observed between the calculated and measured results.

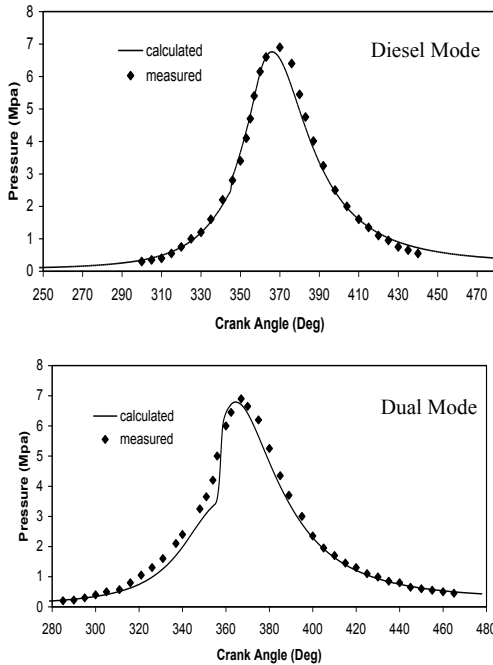


Fig.11: comparison of calculated cylinder pressure in diesel and dual fuel modes with the experimental data.

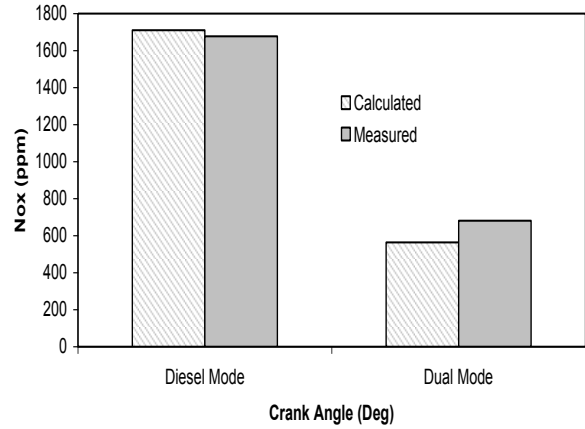


Fig.12: comparison of calculated cylinder NOx in diesel and dual fuel modes with the experimental data.

Figure 13 shows the predicted effect of adding EGR to a direct injected diesel engine on the UHC-NOx tradeoff for different EGR mass fractions. The lower NOx concentration of the 10% EGR case, in comparison with the other EGR cases is evident while the values of UHC at the various EGR mass fractions approximately are constant. It should be notified that the main goal of the present study is to reduce the NOx and soot (the most important emissions from diesel engines) emissions simultaneously. Because the most concern of CI and dual fuel engine emissions is the trade-off between NOx and soot.

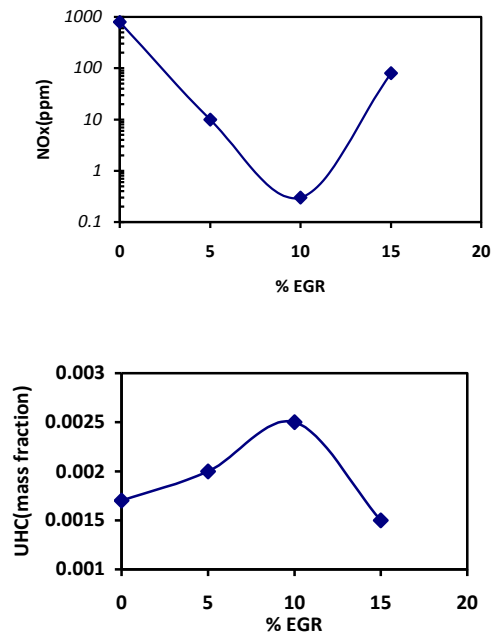


Fig.13: UHC and NO<sub>x</sub> trade off versus different EGR mass fractions.

Figure 13 shows the predicted effect of adding EGR to a direct injected diesel engine on the UHC-NO<sub>x</sub> tradeoff for different EGR mass fractions. The lower NO<sub>x</sub> concentration of the 10% EGR case, in comparison with the other EGR cases is evident while the values of UHC at the various EGR mass fractions approximately are constant. It should be notified that the main goal of the present study is to reduce the NO<sub>x</sub> and soot (the most important emissions at diesel engines) emissions simultaneously. Because the most concern of CI and dual fuel engine emissions is the trade-off between NO<sub>x</sub> and soot.

Figures 6 and figure 7 demonstrate that the 10% EGR case has moved the engine operating condition off the soot-NO<sub>x</sub> tradeoff line for the standard engine, lowering both soot and NO<sub>x</sub> simultaneously. The other cases shifted the engine along the soot-NO<sub>x</sub> trade-off.

#### 4. CONCLUSIONS

At the present work, the effect of EGR on combustion and pollution of a dual fuel engine by CFD code FIRE was investigated. The calculations were at the engine speed of 1400 rpm and full load mode. The EGR percentage was from zero to 15. The results showed that:

- In the case of 15% EGR, the heat release rate becomes higher. The reason is probably due to the activation of the free radicals in the component of EGR gases and their thermal effects that cause the premixed combustion to become higher. Hence, the delay of ignition in the case of 15% EGR is shorter and methane is consumed faster in comparison with the other cases.

- 10% EGR can reduce NO<sub>x</sub> and Soot emissions significantly in comparison with the other cases. Of course, in the 15% EGR case, the emissions were the highest.

- The NO<sub>x</sub> emission is mainly formed close to the bowl of the piston and Soot emission is concentrated to the top of the piston bowl space.

- The predicted values of mean cylinder pressure and NO<sub>x</sub> emission of diesel and dual fuel mode in the normal state condition show a good agreement with the experimental data.

#### 5. NOMENCLATURE

pre exponential factor, area [-]

$A$	
heat flux [W]	$\dot{Q}$
diameter (m)	$d$
fuel consumption rate (kg/s)	$\dot{r}$
energy [kg m <sup>2</sup> /s <sup>2</sup> ]	$E$
stoichiometric; source term [-]	$S$
reaction constant [m <sup>3</sup> /mols]	$K$
temperature [K]	$T$
latent heat of evaporation [J/kg]	$L$
universal gas constant [kJ/mol.K]	$R$
molecular weight [kg/kmol]	
$M$	
mass [kg]	$m$
pressure [p <sub>a</sub> ]	$p$
radius droplet [m]	$r$
relative velocity [m/s]	$u$

#### Greek symbols

wave length [m]	$\Lambda$
heat transfer coefficient [W/m <sup>2</sup> K]	$\alpha$
time scale [s]	$\tau$

#### Subscripts

activation	$a$
formation	$form$
liquid	$l$
soot, surface	$s$
carbon, critical	$c$
fuel	$fu$
natural gas	$NG$
droplet	$d$
forward	$f$
oxidation	$oxid$
fuel vapour	
$f_v$	
gas	$g$
reaction	$R$

#### 6. REFERENCES

- [1] Papagiannakis, R. G., Hountalas, D. T., "Combustion and exhaust emission characteristics of a dual fuel compression ignition engine operated with pilot Diesel fuel and natural gas," *Energy Conversion and Management* 45 (2004) 2971–2987.
- [2] Pirouzpanah, V., Khoshbakhti Saray, R., Sohrabi, A., Niaei, A., "Comparison of Thermal and Radical Effects of EGR Gases on Combustion Process in Dual Fuel Engines at Part Loads," *Energy Conversion and Management* (2007).
- [3] Liu, Z., Karim, G.A., "A Predictive Model for the Combustion Process in Dual Fuel Engines," *SAE Paper* No. 952435, 1995.
- [4] Abd.Alla, G.H., "Using exhaust gas recirculation in internal combustion engines:a review," *Energy conversion and management* 43 (2002) 1027–1042.

- [5] Selim, M., "A Study of Some Combustion Characteristics of Dual Fuel Engine Using EGR," *SAE Paper* No. 2003-01-0766, 2003.
- [6] Anand, R., Mahalakshmi, N., "Simulations reduction of oxides of nitrogen and smoke emissions by using EGR combined with particulate trap in a DI diesel engine," *ASME. ICES2006-1330*.
- [7] Cantore, G., Marco, C., Montorsi, L., Paltrinieri, F., Rinaldini, C., "Analysis of HSDI diesel engine intake system by means of multi-dimensional numerical simulations: Influence of non uniform EGR distribution" *ASME. ICES2006-1359*.
- [8] Lee, S. J., Lee, K. S., Song, S. H., Chun, K. M., "Low pressure loop EGR system analysis using simulation and experimental investigation in heavy-duty diesel engine," *Internal journal of automotive technology* : 659-666 oct 2006.
- [9] Zellat, M.D, Abouri, T, Conte., "Investigation on combustion high EGR level and multiple injection application to DI diesel combustion optimization," *diesel engine emissions reduction conference Chicago-2005*.
- [10] Jones, W., Launder, B., 1972, "The Prediction of Laminarization with a Two-Equation Model of Turbulence. *Int J Heat and Mass Transfer*, vol 15, pp 30.
- [11] Halstead, M., Kirsch, L. and Quinn, C., "The Auto ignition of Hydrocarbon Fueled at High Temperatures and Pressures- Fitting of a Mathematical Model," *Combustion Flame* 30 (1977): 45-60.
- [12] Liu, A. B., Reitz, R. D., "Modeling the Effects of Drop Drag and Break-up on Fuel Sprays," *SAE Paper*, No. 930072, 1993.
- [13] Dukowicz, J. K., "Quasi-Steady Droplet Change in the Presence of Convection," *Informal Report Los Alamos Scientific Laboratory LA7997-MS*.
- [14] Naber, J. D., Reitz, R. D., "Modeling Engine Spray/Wall Impingement," *SAE Paper* No. 88-01-07, 1988.
- [15] Magnussen, B. F., Hjertager, B. H., "On Mathematical Modeling of Turbulent Combustion with Special Emphasis on Soot Formation and Combustion," *Sixteenth International Symposium on Combustion. Pittsburgh: The Combustion Institute*, 1977.
- [16] Nagle, J., Strickland-Constable, R. F., "Oxidation of Carbon between 1000-2000°C", *Proceedings of the Fifth Conference on Carbon*, New York: Pergamon, 1962.
- [17] Pirouzpanah, V et al., "Reduction of pollutants emissions of OM-355 Diesel Engine to Euro2 by converting to Dual-fuel Engine (Diesel / Gas)," *Proceeding of first Conference of Automotive Fuel to CNG*, 19-20 Jun 2003, Tehran, Iran, pp84-94.



---